ECCOMAS Congress 2016
VII European Congress on Computational Methods in Applied Sciences and Engineering
M. Papadrakakis, V. Papadopoulos, G. Stefanou, V. Plevris (eds.)
Crete Island, Greece, 5–10 June 2016

NUMERICAL MODELLING OF COUPLED HYDRO-THERMAL PROCESSES OF THE SOULTZ HETEROGENEOUS GEOTHERMAL SYSTEM

Musa D. Aliyu[1] and Hua-Peng Chen[2*]

[1,2]Department of Engineering Science, University of Greenwich, Chatham Maritime, Kent, ME4 4TB, UK.

[1]M.D.Aliyu@greenwich.ac.uk; *Corresponding author: H.Chen@greenwich.ac.uk

Keywords: Hot Dry Rock, Geothermal System, Supercritical Carbon Dioxide, Heterogeneous, Simulation.

Abstract. *This paper presents an application of the finite element method (FEM) in modelling coupled, hydro-thermal (HT) processes of the Soultz heterogeneous geothermal system, using different working fluids. A two-dimensional (2-D) model of the geothermal system was developed in the Multiphysics FEM application solver (COMSOL), and the geometry comprises of three wells with five geological layers. Also, two discrete fractures were incorporated in the geometry, each with a 2mm thickness. The model mesh consists of various types of elements, including triangular elements, edge elements and vertex elements. The working fluids used in the study were water (H_2O) and supercritical carbon dioxide ($SCCO_2$), using constant density and viscosity. Moreover, other field variables employed in the work were those available in the literature of the geothermal site considered. A long-term simulation of 30 years was applied, and the temperature, pressure, and enthalpy distribution in the production well were studied. The results obtained showed the superiority of water, concerning energy production, when constant density was used. On the other hand, the pressure of the supercritical carbon dioxide in the production wellbore is far superior to that of water. Therefore, supercritical carbon dioxide can serve as a surrogate to water in the future because of its lower pumping cost in comparison to water. Further studies of other parameters are required to affirm the practicability of the scheme.*

1. INTRODUCTION

The thermal energy generated and stored in the earth is called geothermal; the earth's volume has temperatures greater than (>) 1000°C, with only 0.1% at temperatures less than (<) 100°C [1]. The internal structure of our planet and physical processes occurring there are linked with the origin of this heat [2] and also the decay of naturally occurring radioactive isotopes [3]. In the globe, it is estimated that there is 1.45×10^{26} J of geothermal energy, which is equal to 4.95×10^{6} billion tons of standardised coal [4]. The concept of extracting geothermal energy from hot dry rock (HDR) or engineered geothermal system (EGS) is achieved by force circulating fluid between injection and production wells through a naturally fractured rock mass to create a reservoir by hydraulic fracturing [5, 6]. The in situ stress state in the reservoir will perturb as a result of injection/extraction stimulation, which in turn can lead to fracture initiation/propagation and activation of joints and faults [7]. Also, during reservoir stimulation, the interaction between the working fluids and the host rock may result in mineral dissolution/precipitation in the fractures, faults and the wells. Therefore, engineering design is vital to understanding the response of the fractures, faults, and bedding planes to external stresses in HDR reservoirs [8].

Furthermore, projects on this system to date use either water (H_2O) or brine (NaCl) for the reservoir creation and extraction. These substances when dissolved transports mineral species from the system to some parameters such as permeability, porosity, and the wells. For example, calcite and amorphous silica precipitation have caused obstacles in current operating geothermal system at extraction and injection wells, respectively [9]. Water losses in a geothermal reservoir were also part of the critical issues experienced in Rosemanowes site (UK), European geothermal site (France), and many other projects in the Europe and Asia.

Further to the problems mentioned above experienced using those working fluid in the systems, a novel approach was proposed by Brown [10] to replace H_2O with supercritical carbon dioxide ($SCCO_2$) for both reservoir creation and heat extraction. The study, reported by Pruess [11], reveals that $SCCO_2$ offers larger compressibility and expansivity compared to water. Also using $SCCO_2$ in a closed-loop geothermal reservoir as a substitute for water offers three significant advantages as mentioned by Brown [9] . If $SCCO_2$ is utilised as the circulating fluid in HDR reservoirs, the fluid losses experienced will serve as geological storage of the CO_2. Previous research conducted on this topic were on homogenous hot dry rock (HDR) system, but, however, the systems were heterogeneous in nature. This paper compared the use of $SCCO_2$ and H_2O as working fluid in the heterogeneous geothermal system located at Soultz (France) using the finite element method (FEM).

1.1 Overview of the Soultz Geothermal System

The Soultz site in France was initiated by the European Commission after a detailed surveyed conducted on the three most foremost geothermal projects in Europe that include Rosemanowes, Bad Urach and Soultz to get a commercialised geothermal site within the Europe. A decision was made in 1987 to locate the site in the Soultz, France, due to volcanic activities experienced in the vicinity of a petroleum reservoir site. The project received its initial funding from the European Commission and the relevant energy ministries of France, Germany, and the United Kingdom. Scientist and engineers of these countries established a permanent base on the site to coordinate the activities of various research teams from the participating countries and also to plan the work [12]. Other nations also joined the project later; these countries include Italy, Switzerland and most recently Norway. The United States and Japan

have also made their contributions from the research. The project has undergone four different stages, but only the last phase will be considered here.

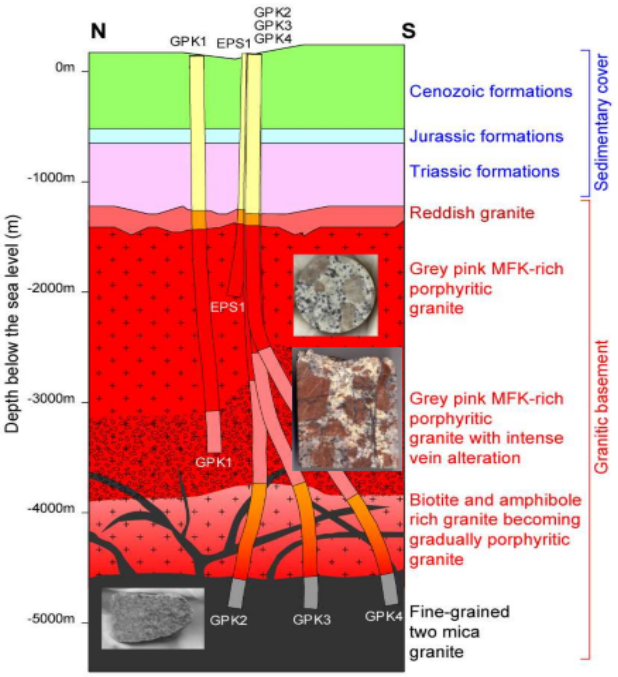

Figure 1: Geological Formation of Geothermal Reservoir at Soultz-Site (France) [13].

Figure 1 represents the geological formation of the entire system and Figure 2 characterises the temperature gradient of the system. The temperature profile is divided into three core zones. The upper zone has a geothermal gradient of 110ºC/Km. The intermediate and the lower zone attribute geothermal gradient of 5ºC/Km and 30ºC/Km, respectively.

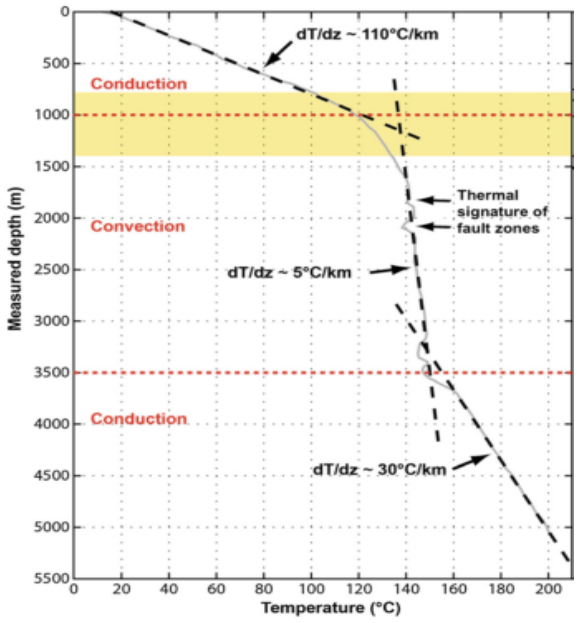

Figure 2: Equilibrium Temperature Profile Obtained from GPK-2 [14].

Moreover, the system wells arrangements are also depicted in Figure 3. GPK3 is the injection well, GPK2 and GPK4 are the production wells. EPS1 and GPK1 are the previous wells used in the earlier stage of the project.

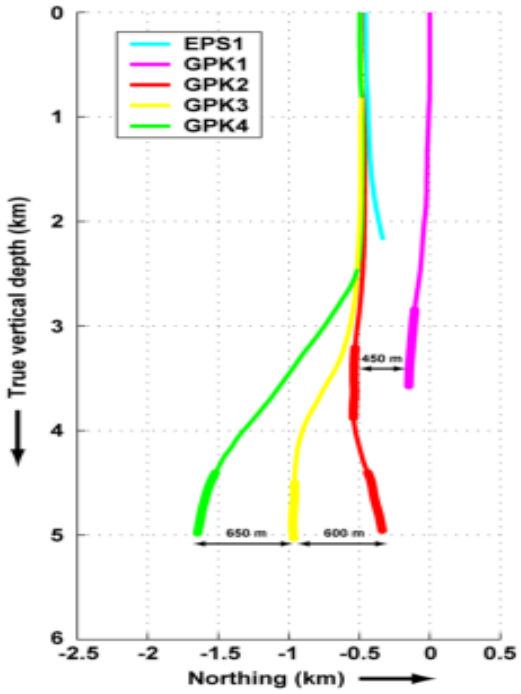

Figure 3: Well Arrangements at Soultz Site (South-North Vertical Cross-Section) [15].

2. MATHEMATICAL AND FINITE ELEMENT FORMULATION OF THE PROBLEM

2.1 Mathematical Formulations

This section gives an exposition of the equations applied in the study. The first set of the equation is based on the law of conservation of mass and is used for the hydraulic process with the assumption that the flow obeys Darcy's law for free movement and is given here as,

$$\rho S \frac{\partial P}{\partial t} + \nabla \cdot \rho \left[\frac{-\kappa}{\mu} (\nabla P + \rho g) \right] = Q_M \tag{1}$$

where ρ is the density, S represents the storativity, P is the pressure, ∇ is the shorthand for the first derivatives with respect to the dimensions of the problem, κ denotes the permeability, μ is the dynamic viscosity, g represents the acceleration of gravity, t is the time and Q_M represent the source term. The second set of the equation is the energy balance equation for heat transport in porous media by considering the Fourier's law of heat flux is expressed as,

$$\rho C_P \frac{\partial T}{\partial t} + \rho C_p v \cdot \nabla T = \nabla \cdot (\lambda \nabla T) + Q \tag{2}$$

where C_p is the specific heat capacity, T represents the temperature, v is the convective term for the velocity, λ denotes the thermal conductivity and Q is the heat source term. The permeability model in the equation (1) can also be replaced by hydraulic conductivity model, and the relationship between the two are:

$$K = \frac{\kappa \rho g}{\mu} \qquad or \qquad \kappa = \frac{K\mu}{\rho g} \tag{3}$$

in which K represents the hydraulic conductivity. The third set of the equation deals with the fracture properties. Equation (4) is the fracture permeability equation govern by the cubic law with the assumption of laminar flow between two parallel plates which is given as,

$$\kappa_{fr} = \frac{a^2}{12} \tag{4}$$

where K_{fr} denotes the fracture permeability, a represents the fracture aperture. Blöcher [16] relates the fracture transmissibility to the aperture and permeability, expressed as,

$$TR_{fr} = \kappa_{fr} a \qquad or \qquad a = \sqrt[3]{12\,TR_{fr}} \tag{5}$$

where TR_{fr} denotes the fracture transmissibility, and by substituting left-hand side of (5) into (4) yields the right-hand side of (5), which is referred as the fracture aperture. The Darcy's and Fourier's flux in equations (1) and (2) can also be expressed as,

$$q_h = -\frac{k}{\mu}\left[\nabla P + \rho g\right] \qquad and \qquad q_T = -\lambda \nabla T \tag{6}$$

2.2 Finite Element Method

This section presents the application of finite element method (FEM) to coupled thermo-hydraulic (TH) problems in discretely fractured porous media. The partial differential equations (PDE) used were already described in the previous section.

2.2.1 Weak Formulation

The Green's theorem and the Method of Weighted Residuals (MWR) were applied to the governing equations provided in the previous section to derive weak formulation of the problem. The weak forms for the mass conservation equation (1) and the energy balance equation (2) are expressed as,

$$\int_{\Omega} w\rho S \frac{\partial P}{\partial t} d\Omega - \int_{\Omega} \rho \nabla w^T \cdot q_h d\Omega + \int_{\Gamma_h^q} w\rho (q_h \cdot n) d\Gamma - \int_{\Omega} w Q_m d\Omega = 0 \tag{7}$$

$$\int_{\Omega} w\rho C_P \frac{\partial T}{\partial t} d\Omega + \int_{\Omega} w\rho C_p v \cdot \nabla T d\Omega - \int_{\Gamma_T^q} w(q_T \cdot n) d\Gamma - \int_{\Omega} w^T Q d\Omega = 0 \tag{8}$$

where Ω and Γ represents the model domain and boundary, w is the weighting function, n is the normal to the boundary, subscript and superscript T denotes the thermal and transpose, respectively. The boundary conditions are specified for all field functions P and T.

2.2.2 Galerkin FEM Formulations

The weak forms (7) and (8) of the TH balance equations were spatially discretised using the standard Galerkin Method. Primary variables were fluid flow pressure P and temperature T, which were approximated by interpolation functions

$$P^y = N_P P \tag{9}$$

$$T^y = N_T T \tag{10}$$

where P and T were the scalars of the nodal values of the unknowns. N_P and N_T were the shape functions for P and T, respectively. The finite element formulation of the governing equations were given in a matrix form as,

$$M_h^m P'^m + K_h^m P^m - q_h^m = 0 \tag{11}$$

$$M_T^m T'^m + K_T^m T^m - q_T^m = 0 \tag{12}$$

where M and K were process-specific mass and stiffness, respectively. The term q contained the contributions of the coupled processes. The process-specific matrices for the fluid flow and thermal are given in equations (13), (14), (15), (16), (17), and (18) and same can be written as,

$$M_h^m = \int_\Omega N_P^T \rho S N_P d\Omega \tag{13}$$

$$K_h^m = \int_\Omega \nabla N_P^T \frac{\kappa}{\mu} \nabla N_P d\Omega \tag{14}$$

$$q_h^m = -K_h^m \rho g - \int_{\Gamma_q} N_P^T q d\Gamma \tag{15}$$

$$M_T^m = \int_\Omega N_T^T C_P \rho N_T d\Omega \tag{16}$$

$$K_T^m = \int_\Omega N_T^T C_P \rho v \cdot \nabla N_T d\Omega + \int_\Omega \nabla N_T^T \lambda \nabla N_T d\Omega \tag{17}$$

$$q_T^m = \int_\Gamma N_T^T q_T \cdot n d\Gamma + \int_\Omega N_T^T Q d\Omega \tag{18}$$

3. PROBLEM DESCRIPTION AND IMPLEMENTATION

3.1 Geometry, Mesh and System Properties

A two-dimensional model of the geothermal system is developed based on the above FEM procedures. The model geometry is depicted in Figure 4; it is comprised of three wells with five geological layers as discussed earlier in the previous section. Also, two discrete fractures are inputted in the geometry with 2 mm thickness each. The model mesh is shown in Figure 5, consisting of 1,973 triangular elements, 409 edge elements, and 48 vertex elements. Furthermore, geological properties and densities of the system are also presented in Table 1 [17]. Other field variables applied in the model are provided in Table 2 as determined by [18]. Other parameters used are given in the literature of Brown [10] and Pruess [11].

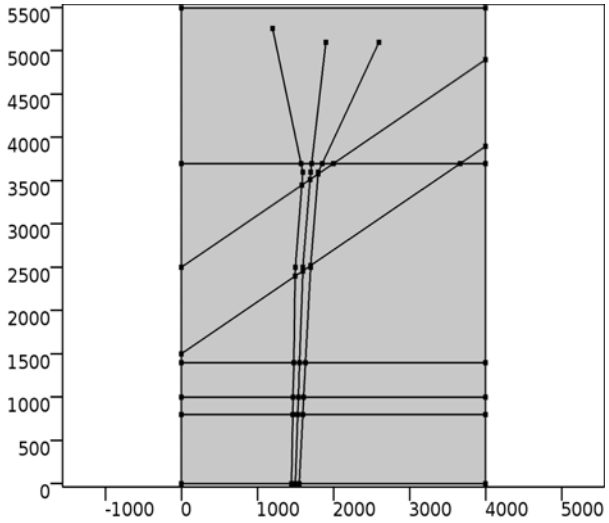

Figure 4: Model Geometry

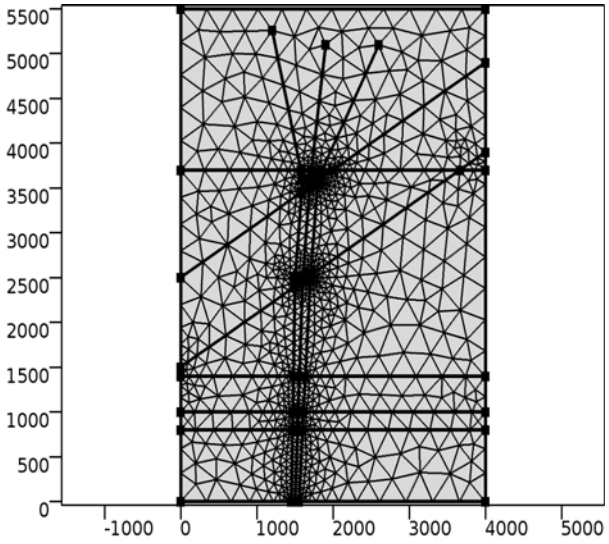

Figure 5: Model Mesh

Formation	Depth (km)	Density (kg/m^3)
Tertiary	0 - 0.75	2350
Jurassic	0 - 0.75	2550
Keuper	0.75 - 0.85	2700
Muschelkalk	0.85 - 1.0	2700
Bunstsandstein	1.0 - 1.4	2500
Basement	1.4 - 5.5	2600

Table 1: Geological Properties and Densities at Soultz (France)

Depth (km)	Permeability (m^2)	Porosity (%)	Thermal Conductivity (W/m/K)
0 - 0.8	10^{-17}	15	1.4
0.8 - 1.0	10^{-16}	15	2.1
1.0 - 1.4	5×10^{-15} - 10^{-14}	15	2.5
1.4 - 3.7	3×10^{-15}	9	3.0
3.7 - 5.0	10^{-18}	1	3.0
Faults	10^{-17} - 3×10^{-14}	15	2.5

Table 2: The Petro-Physical Properties of Main Lithological Formations at Soultz EGS.

3.2 Initial and Boundary Conditions

The initial temperature of the system is given as,

$$T_0 = T_{surf} - b(-z) \tag{19}$$

where T_0 is the initial temperature, T_{surf} denotes the surface temperature, and a value of 10ºC is applied in this study, b is the geothermal gradient, an average gradient of 30ºC/km is used, and z is the depth of the system from the surface. The initial pressure is taken as a constant hydrostatic pressure of 51 MPa. On the other hand, the boundary condition applied is the Dirichlet type (i.e. fixed boundary condition) on well GPK3, in other words, injection well and it corresponds to the temperature and the pressure of 50ºC and 45 MPa respectively.

The simulation was for 30 years, because of the relatively long simulation time and the stability afforded by the constant pressure and temperature conditions. A time-dependent solver BDF (Backward Difference Formula) was employed in COMSOL, and the number of degrees of freedom (DOF) adopted was 5050 (plus 870 internal DOFs). The scheme has an advantage of limiting time step. In this case, it took only 34-time steps to model the 30-year production. The physical computer memory used for the solution is 963 MB and a virtual memory of 1042 MB.

4. RESULTS AND DISCUSSIONS

In this study, a finite element model is developed for the Soultz heterogeneous geothermal system using different working fluids. The first sets of the results presented are the pressure distribution along the geothermal system as shown in Figure 6. Figure 6a presents the pressure distribution in the system after one year of simulation. As can be seen from the illustration, part of the sedimentary layers has a significant drop in the pressure due to the nature of binding between the grains, which leads to an earlier formation of hydraulic fractures within the layers. After additional pumping for 10 years, a total drop in the pressure of the sedimentary layers is observed, as shown in Figure 6b.

Furthermore, Figures 6c and 6d presents the distribution of the pressure for 20 and 30 years of simulation. As seen from both figures the pressure drawdown has less effect on the sedimentary layers due to complete formation of hydraulic fractures in the entire system.

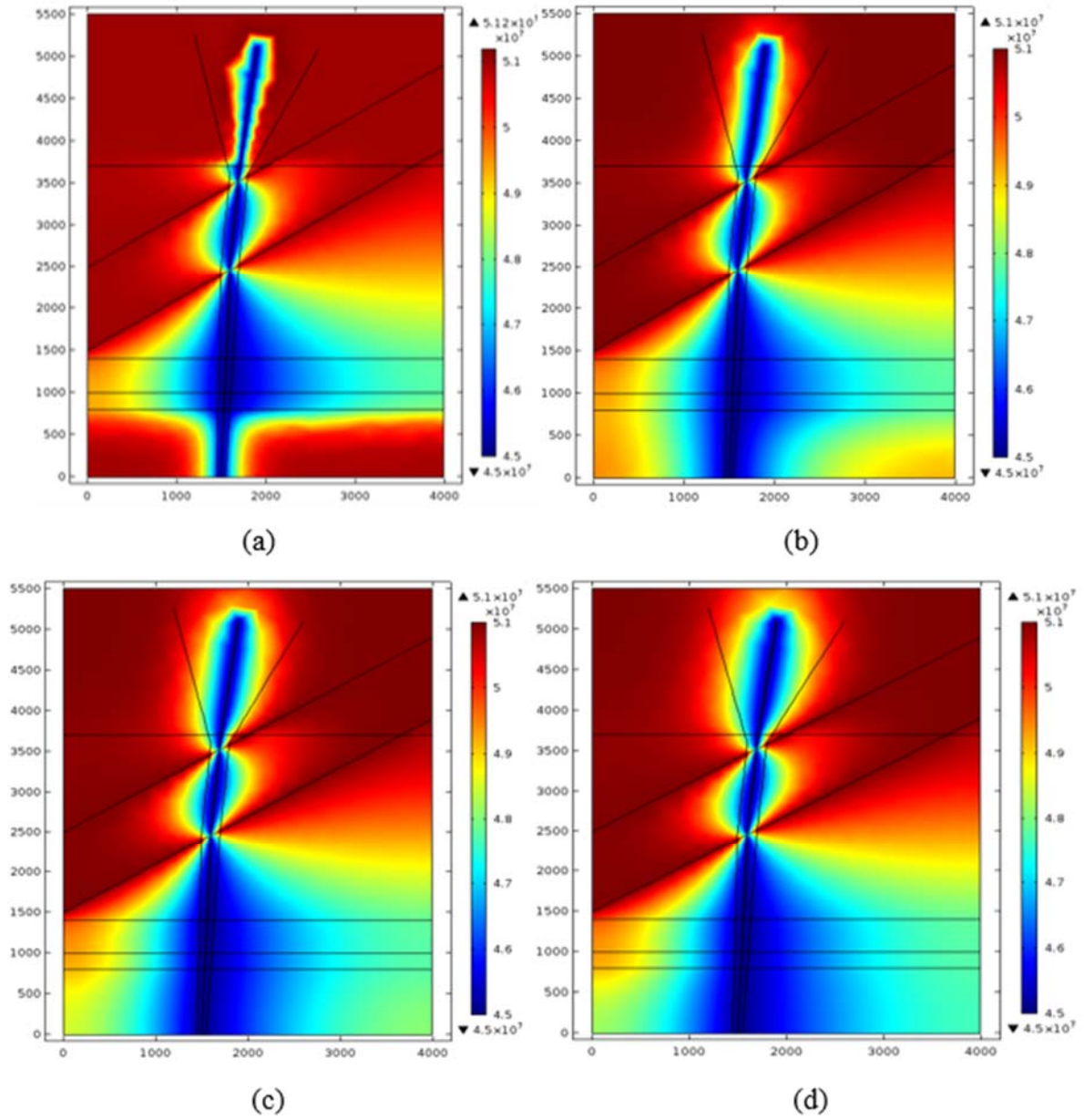

Figure 6: (a) Pressure (MPa) Distribution after 1 Year, (b) Pressure (MPa) Distribution after 10 Years, (c) Pressure (MPa) Distribution after 20 Years, and (d) Pressure (MPa) Distribution after 30 Years

The second set of results analysed in this study includes the production temperature, enthalpy, and pressures at the wellhead of the system. Figure 7 presents the temperature produced at the wellhead, and as can be observed, a drawdown from the initial system temperature of 200°C to 198.8°C is observed after six years of simulation for the $SCCO_2$. On the other hand, a drawdown from 200°C to 198.9°C is observed after seven years of simulation for the H_2O. Also, after 30 years of simulation, the wellhead temperatures for the H_2O at wells, GPK2 and GPK4, are 168.6°C and 165.8°C, respectively. However, in the case of the $SCCO_2$, the wellhead temperatures are 162.9°C and 160°C, respectively.

Figure 8 presents the production pressure of the system under 30 years of simulation. As it can be observed, the pressure produced at the wellhead after one year of simulation is 46

MPa for the H_2O and 50.8 MPa for the $SCCO_2$. Also, the least produced pressure by the $SCCO_2$, at 30 years, is 46.7 MPa, which is greater than the highest produced pressure by the H_2O.

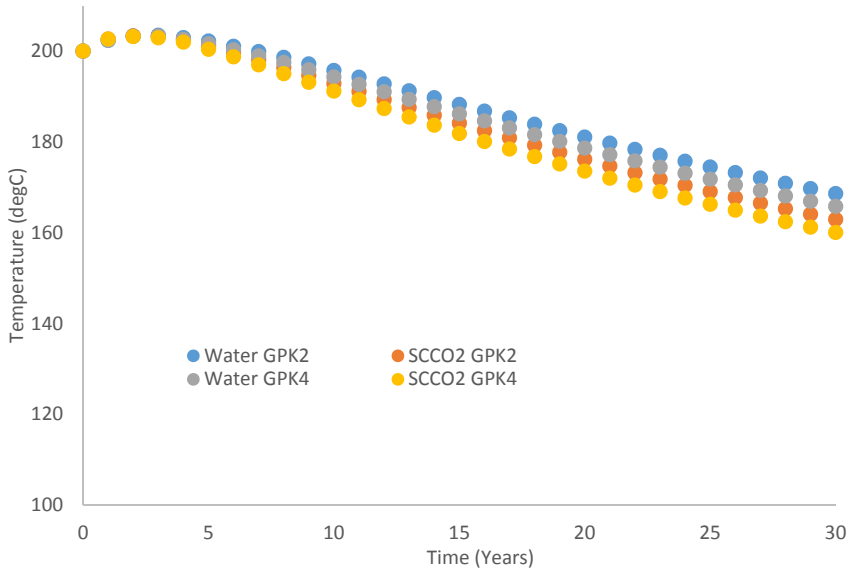

Figure 7: Temperature at the Production Wells

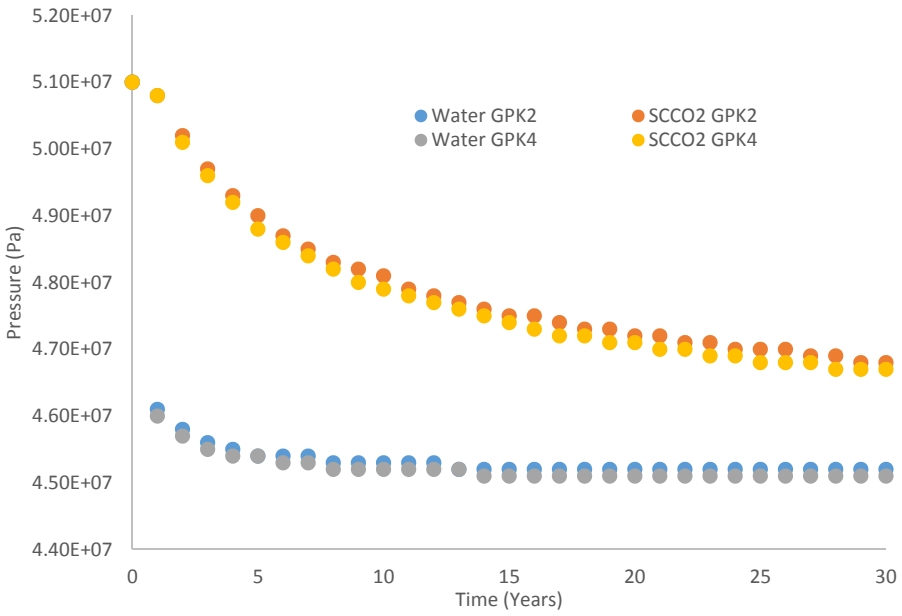

Figure 8: Pressure at the Production Wells

Figure 9 presents the enthalpy produced at the wellhead. As seen, the drawdown pattern is similar to that of the temperature scenario, but the difference in the values obtained for both the working fluids is higher. The maximum produced enthalpy for the H_2O is 748.4 kJ/kg at three years of simulation while that of the $SCCO_2$ is 570.3 kJ/kg at two years of simulation. The least produced enthalpy by the H_2O, which is 590.5 kJ/kg at 30 years, is greater than the maximum produced by the $SCCO_2$. However, the same is observed in the pressure results but

in the reverse order. This occurs because of the relationship between the two parameters, which is expressed as

$$H = U + pV \tag{19}$$

where H, U, p, and V are the total enthalpy, energy of the work done in the system, pressure, and volume of the system, respectively. The above expression, from system thermodynamics, confirms the analysis performed on these parameters to be true.

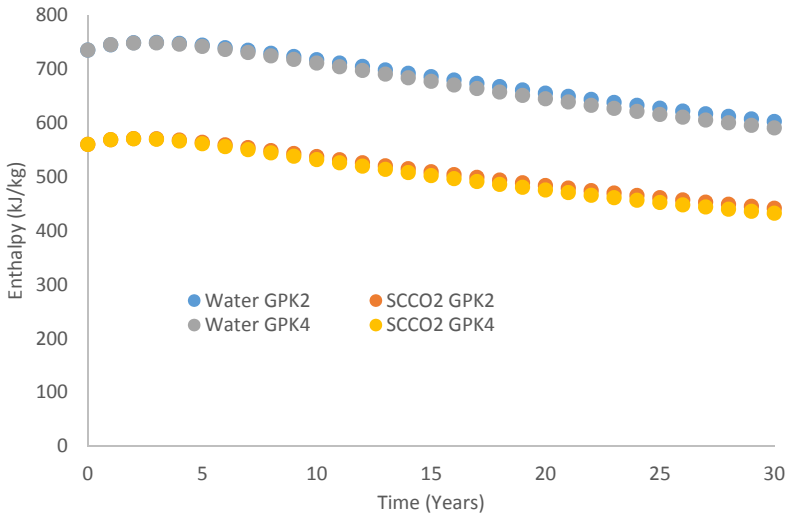

Figure 9: Enthalpy at the Production Wells

5. CONCLUSIONS

A coupled, thermo-hydraulic solution of a heterogeneous, geothermal system is presented, using water and supercritical carbon dioxide as the working fluids. The model takes into account non-isothermal, single-phase flow in porous media connected to discrete fractures. The results of present study show that H_2O is superior to $SCCO_2$, regarding energy extraction (i.e., in cases of temperature and enthalpy), but $SCCO_2$ is produced at a higher pressure at the production wells and reaches larger overall flow rates than H_2O. The difference concerning temperature is of less significance than that of enthalpy, which is quite substantial. On the other hand, the pressure of $SCCO_2$ at the production wells is higher than water because the buoyancy properties of $SCCO_2$ is greater than that of H_2O. The study also affirms the possibility of replacing the $SCCO_2$ with H_2O in the future.

REFERENCES

[1] P. Bayer, L. Rybach, P. Blum, and R. Brauchler, "Review on life cycle environmental effects of geothermal power generation," *Renew. Sustain. Energy Rev.*, vol. 26, pp. 446–463, Oct. 2013.

[2] E. Barbier, "Geothermal energy technology and current status: an overview," *Renew. Sustain. Energy Rev.*, vol. 6, no. 1–2, pp. 3–65, Jan. 2002.

[3] M. Brunner, H. L. Gorhan, and L. Rybach, "GEOTHERMAL ENERGY : Plentiful and Environmentally Friendly," Germany, 2015.

[4] Y. Huang, S. Ren, and D. Zhang, "Current Status and Developing Trend of Direct Use in Global Geothermal Resource," in *Fortieth Workshop on Geothermal Reservoir Engineering Stanford University, Stanford, California, January 26-28, 2015 SGP-TR-204*, 2015, pp. 1–8.

[5] D. W. Brown and D. V Duchane, "Scienti progress on the Fenton Hill HDR project since 1983," *Geothermics*, vol. 28, no. 4, pp. 591–601, 1999.

[6] J. Willis-Richards and T. Wallroth, "Approaches to the modelling of hdr reservoirs: A review," *Geothermics*, vol. 24, no. 3, pp. 307–332, 1995.

[7] A. Ghassemi, S. Tarasovs, and A. H.-D. Cheng, "A 3-D study of the effects of thermomechanical loads on fracture slip in enhanced geothermal reservoirs," *Int. J. Rock Mech. Min. Sci.*, vol. 44, no. 8, pp. 1132–1148, Dec. 2007.

[8] J. Taron and D. Elsworth, "Coupled mechanical and chemical processes in engineered geothermal reservoirs with dynamic permeability," *Int. J. Rock Mech. Min. Sci.*, vol. 47, no. 8, pp. 1339–1348, Dec. 2010.

[9] J. Taron and D. Elsworth, "Thermal–hydrologic–mechanical–chemical processes in the evolution of engineered geothermal reservoirs," *Int. J. Rock Mech. Min. Sci.*, vol. 46, no. 5, pp. 855–864, Jul. 2009.

[10] D. Brown, "a Hot Dry Rock Geothermal Energy Concept Utilizing Supercritical Co2 Instead of Water," *Twenty-Fifth Work. Geotherm. Resevoir Eng.*, vol. 1995, no. April 1992, pp. 1–6, 2000.

[11] K. Pruess, "Enhanced geothermal systems (EGS) using CO2 as working fluid-A novel approach for generating renewable energy with simultaneous sequestration of carbon," *Geothermics*, vol. 35, no. 4, pp. 351–367, 2006.

[12] D. Duchane, "The History of HDR Research and Development," in *Proceedings, 4th International HDR Forum, Strasbourg, France, September 28-30, 1998*, 1999, no. 836.

[13] P. Schlagermann, "Overview of the Soultz geothermal project Overview of the Soultz geothermal project," no. 3. pp. 66–75, 2011.

[14] J. Vidal, A. Genter, and J. Schmittbuhl, "How do permeable fractures in the Triassic sediments of Northern Alsace characterize the top of hydrothermal convective cells? Evidence from Soultz geothermal boreholes (France)," *Geotherm. Energy*, vol. 3, no. 1, 2015.

[15] A. Genter, X. Goerke, J. Graff, N. Cuenot, G. Krall, M. Schindler, and G. Ravier, "Current Status of the EGS Soultz Geothermal Project (France)," *World Geotherm. Congr.*, vol. C, no. April, pp. 25–29, 2010.

[16] M. G. Blöcher, M. Cacace, B. Lewerenz, and G. Zimmermann, "Three dimensional

modelling of fractured and faulted reservoirs: Framework and implementation," *Chemie der Erde - Geochemistry*, vol. 70, no. SUPPL. 3, pp. 145–153, 2010.

[17] P. Baillieux, E. Schill, Y. Abdelfettah, and C. Dezayes, "Possible natural fluid pathways from gravity pseudo-tomography in the geothermal fields of Northern Alsace (Upper Rhine Graben)," *Geotherm. Energy*, vol. 2, no. 1, p. 16, 2014.

[18] L. Guillou-Frottier, C. Clément, B. Bourgine, V. Bouchot, and A. Genter, "Hydrothermal convection beneath an inclined basement-sediment interface : application to the Rhine graben and its Soultz-sous-Forêts temperature anomaly Case of impervious faults Case of permeable faults," in *AGU Fall Meeting, San Franscisco, 3-7 December, 2012*, 2012, p. 1.